International Journal of Thermal Sciences 155 (2020) 106417

Contents lists available at ScienceDirect

International Journal of Thermal Sciences

journal homepage: http://www.elsevier.com/locate/ijts

Design optimization of a shell-and-tube heat exchanger with novel three-zonal baffle by using CFD and taguchi method

Nihat Biçer [a], Tahsin Engin [a,*], Halit Yaşar [a], Ekrem Büyükkaya [a], Ahmet Aydın [b], Adnan Topuz [c]

[a] Sakarya University, Engineering Faculty, Mechanical Engineering Department, Sakarya, Turkey
[b] Sakarya University, Research-Development&Application Center-SARGEM, 54200, Sakarya, Turkey
[c] Bülent Ecevit University, Faculty of Engineering, Department of Mechanical Engineering, 67100, Incivez, Zonguldak, Turkey

ARTICLE INFO

Keywords:
Shell-and-tube heat exchanger
Optimization
Three-zonal baffle
Taguchi method

ABSTRACT

In this study, a novel and innovative baffle design was offered in order to considerably reduce shell side pressure loss without compromising thermal performance. Computational fluid dynamics (CFD) was utilized to simulate and visualize 3-D turbulent flow field in the shell side so as to investigate various shapes of baffles for preliminary baffle design purposes. The simulation results showed that a so-called three-zonal baffle could be superior over the several other configurations considered. The set of design parameters was then identified for this shape of baffle and Taguchi method was employed to determine candidate design configurations for optimum. With the optimized design of shell-and-tube heat exchanger (STHE) with new baffle configuration, it was found that thermal performance of the heat exchanger with three-zonal baffles was slightly improved, whereas shell-side pressure drop was significantly decreased compared to the conventional baffled STHE. The shell side pressure loss was found to lower by 49%, accompanying an increase in the shell side temperature difference up to 7%. In addition, CFD analyses of the optimized STHE with three-zonal baffles were performed considering specific boundary conditions, and the results were validated with the experimental data obtained under the same conditions. The results showed that the differences between CFD analyses and experimental data were maximum 7.3% for heat transfer rate and 7.6% for the pressure drop. It was concluded that the three-zonal baffles improved the STHE performance in terms of both heat transfer rate and pressure loss points of view.

1. Introduction

Heat exchangers are devices used for transferring thermal energy between a solid object and a fluid, or between two or more fluids. The fluids may be separated by a solid wall to prevent mixing or they may be in direct contact. They are widely used in space heating, refrigeration, air conditioning, power stations, petrochemical, chemical, and pharmaceutical industries, natural gas processing and wastewater treatment [1]. Among these, STHEs are the most commonly used ones. In this system, heat transfer performance depends on many parameters such as layout of tubes on the tubesheet, number of baffles, number of tubes and length. It is possible to improve the performance of a heat exchanger by changing baffle geometry. Changing the baffle geometry has significant effects on the flow characteristics and heat transfer on the shell side. The traditional STHE with segmental baffles are described by high pressure drop, leakage flow in large amount, stagnant flow zones, becoming dirty and flow induced vibration at high speeds [2,3].

The tube used in the heat exchanger plays an important role in energy transfer. For this reason, many research studies have been carried out for heat exchanger tube developed by using heat improvement techniques. The efforts to improve the performance of heat exchangers are still in progress [4–6]. The development of heat transfer in the heat exchanger using different geometric models still maintains the agenda. The only thing targeted in all the different geometries used is to change the physical behavior of the fluid flow to increase the heat transfer. Although there are different geometric shapes of heat exchangers, the STHE has more application areas than the others due to the wide range of operating temperature and pressure [4–7]. There are many studies in the literature to improve the performance of STHEs. An important part of these studies focuses on baffle design. For this purpose, many innovations such as new baffle design, new baffle configuration have been carried out. Examples of some new types of baffles that are being studied to improve the performance of Shell and tube heat exchangers are trefoil-hole baffle [8–10], helical baffle [11–22], flower baffle [8,16,23,24], staggered baffle [23,25], trapezoidal baffle [26], ladder-type fold

* Corresponding author. University of Sakarya, Engineering Faculty, Mechanical Engineering Department, 54187, Esentepe Campus Serdivan-Sakarya, Turkey.
E-mail address: engint@sakarya.edu.tr (T. Engin).

https://doi.org/10.1016/j.ijthermalsci.2020.106417
Received 10 September 2019; Received in revised form 24 March 2020; Accepted 8 April 2020
Available online 30 April 2020

Nomenclature

A	distance between the baffles (mm)
B	rotation angle of the baffle (degree)
C	ratio of outer diameter to inner diameter of the baffle
c_p	specific heat of the fluid (kJ/kg-K)
CFD	Computational Fluid Dynamics
D	angle of openness to center (degree)
E	ratio of openness to closure
$\dot{m}$	mass flow rate (kg/s)
$\dot{Q}$	heat transfer rate (kW)
K	coverage factor
SHTE	Shell-and-Tube Heat Exchanger
S/N	Signal/Noise ratio
S^2	variance of observed values
ΔT	temperature difference (K)
U	uncertainty (%)
$\bar{y}$	average of observed values
y_i	performance characteristics of the performance
Subscript	
Ins	instrument
rep	repeatability

baffles [27], clamping baffle [28,29], round rod baffle [28,30] and louwer baffle [31]. Leoni et al. [32] investigated the effect of baffle clearances on a shell and tube heat exchanger performance. Their results showed that the pressure drop was about 40% smaller when clearances were considered. Mellal et al. [33] investigated a three-dimensional numerical simulation of turbulent fluid flow and heat transfer in the shell side of a shell and tube heat exchanger. They tested two primordial parameters: baffles spacing of 106.6, 80 and 64 mm and six baffles orientation angles of 45°, 60°, 90°, 120°, 150° and 180°. Their results showed that the baffle orientation angle of 180, at 64 mm of baffle spacing was the best design. Arania and Moradi [34] focused on the fluid flow and heat transfer of water inside the segmental baffle shell and tube heat exchanger optimization using combined baffle and longitudinal ribbed tube configuration. At maximum mass flow rates (2 kg/s), the average value of shell-side heat transfer coefficient of disk baffle shell and tube heat exchanger and combined segmental-disk baffle shell and tube heat exchanger were 26.6% and 31.9% higher than disk baffle shell and tube heat exchanger with longitudinal circular ribbed tube and combined segmental-disk baffle shell and tube heat exchanger with longitudinal circular ribbed tube, respectively.

Baffle range and baffle gap are an important parameter in the design of the STHEs. If the baffle spaces are left larger or smaller than the optimum design, they usually result in large vortices of poorly distributed flow, dead zones, and higher pressure losses than expected. Determination of these parameters by experimental methods also causes a significant amount of material waste. In addition, it is very difficult to investigate the effect of each parameter on heat conduction, flow resistance and thermo-hydraulic performance on the shell side. Therefore, some optimization methods are used to reduce the number of experiments and their costs. One of them is Taguchi optimization method. Taguchi method is an experimental design method based on parameter, system and tolerance design. This method is widely used in statistical analysis of data collected within the scope of quality assurance systems. However, it is also a very useful method to determine the optimal combination between different levels of different parameters. Thus, it is possible to reach a much less number of experiments by using the Taguchi method in cases where too much experimental work is required to determine the effect of each parameter [35].

In the literature, there are some studies performed by applying Taguchi method in heat exchangers. Gunes et al. [36] applied the Taguchi optimization method for copper coil heat exchanger design parameters. They used this method to determine the optimization of heat transfer with minimum pressure drop. Similarly, Chamoli [37] also worked on the optimization of flow and geometric parameters in a rectangular channel roughened with V geometry baffles using Taguchi for the same purpose. The selected parameters for performance prediction of V down perforated baffle roughened rectangular channel were relative roughness pitch, relative roughness height, open area ratio and Reynolds number. Tang et al. [38] investigated the effects of the vortex generator fin-tube heat exchanger parameters have been optimized with the Taguchi method. The levels of each factor were combined to form sixteen models and analyze the heat transfer and flow friction characteristics of each model. Another similar study was done by Zeng et al. They examined the parameters of vortex-generator fin-and-tube heat exchangers, such as attack angle, length of vortex generator, height of vortex generator, fin material, fin thickness, fin pitch and tube pitch by the Taguchi method [39]. Aghaie et al. [40] investigated on optimized geometry of angled ribs for enhancing the thermohydraulic behavior of a solar air heater channel by Taguchi method. They were used L_{16} orthogonal array to optimize the geometry factors accounts for the maximum thermal performance of the ribbed channel. Tingting et al. [41] investigated the influence of helix angle, overlap size, diameter of tube, central distance of tube and tube layout on the performance of overlapped helical baffled heat exchangers using Taguchi method. Sivasakthivel et al. [42] used Taguchi method to carry out the parametric optimization for heating or cooling mode operation. Etghani and Baboli [43] investigated heat transfer coefficient and exergy loss. In their study, four design parameters (pitch coil, tube diameter, hot and cold flow rates) were considered and Taguchi method were used to obtain the optimum levels of the design factors. Zhang et al. [44] investigated the effect of the structural parameters of three-dimensional finned tubes on the heat transfer and pressure drop characteristics in the air cross-flow by the Taguchi method to improve the heat transfer efficiency. Chamoli et al. [45] used Taguchi grey relational analysis method approach for the multi response optimization of different geometrical and flow parameters on thermo-hydraulic performance of heat exchanger tube with perforated disk insert. They concluded that the most significant parameter with respect to grey relational analysis was diameter ratio. Miansari et al. [46] optimized a helically grooved shell and tube heat exchanger by using Taguchi experimental design method. They investigated the performance of the heat exchanger for different working conditions, such as different level of cold fluid inlet temperature, cold fluid flow rate, and groove height. They concluded that the optimum groove height was 10 mm.

In this study, it is aimed to improve the performance of shell-and-tube heat exchangers by using a new baffle design. For this aim, a three-zonal baffle has been proposed to use in shell and tube heat exchangers. As a result of the investigations, it was found that there were no studies performed using this type of baffle in the literature. Using these new three-zonal baffles, it is ensured that the fluid in the shell-side is more effectively mixed by creating a propeller effect leading to relatively higher convective heat transfer coefficient. Thus, it is intended to direct the fluid towards the shell walls by striking the baffles. The heat exchanger with three-zonal baffles was then optimized by using the Taguchi experimental design method considering the heat transfer rate and pressure drop. The optimized heat exchanger was then manufactured and tested. The experimental results were compared to CFD results, and it was found that a good agreement between measured and simulated results exist. Overall, the results showed that the STHE with new baffle design lead to considerable lower pressure drop in the shell-side with an improved thermal performance.

2. CFD analyses

In this study, a new type three-zonal baffle has been developed for the STHEs. CFD analyzes of the heat exchanger with three-zonal baffle were then performed and the obtained results were compared to the results of the heat exchanger with conventional baffles. CFD analyses were performed for two different mass flow rates, one low and one high. In the first case, the mass flow rates of hot water passing through the tubes, and mass flow rates of cold water passing through the shell were taken as 0.5 kg/s and 0.25 kg/s, respectively. On the other hand, in the second case, the mass flow rates of hot and cold water were taken as 2.88 kg/s and 2.19 kg/s, respectively. The inlet temperatures of hot and cold water were taken as 77 °C and 15 °C, respectively. Table 1 shows the properties of the fluids flowing through the heat exchanger.

The flow geometry was modeled with the separate ANSYS Design Modeler for the conventional and three-zonal baffle model. In these models, two separate control volumes were modeled to analyze shell-and-tube side flows. The heat exchangers with three-zonal and conventional baffles are shown in Fig. 1. On the other hand, geometric dimensions of the conventional and three-zonal baffles are given in Fig. 2.

In this study, a small STHE for CFD simulations was modeled. A commercial CFD package, namely ANSYS Fluent was used for numerical computations. Since the flow in the tube-side is well-established both experimentally and theoretically, the current study focused on the tube-side flow. Table 2 gives the heat exchanger specifications.

The standard k-ε turbulence model was used in the CFD analyses. Tetrahedral elements were used and the number of elements was taken as 7,045,950. Fig. 3. Shows element number independency of the numerical solution based on pressure drop and temperature difference. As can be seen from the figure, when the number of elements is increased by more than 7,045,950, there is no change in the values obtained from the analyses. The overall view of the mesh structure is shown in Fig. 4. In order to model the tube surface fouling resistance, thermal conductivity was taken as 3.36 W/m-K at the interface. The simulations were performed on a DELL T5600 Workstation (Intel® Xeon®, 3.30 GHz, 2 processors, 16 cores, 128 GB RAM). The solution time was about 18 h for each solution.

3. Taguchi optimization

In this study, Taguchi Experimental Design method was used to optimize the STHE with new design three-zonal baffles. Detailed information about Taguchi method is available elsewhere in the literature and therefore we will not provide here any mathematical background of this method. Therefore, this section is more concerned with the adaptation of the Taguchi method to the study.

Experimental optimization of the STHEs by Taguchi method consists of three main steps: System design, parameter design and tolerance design. In the system design step, it is aimed to determine the parameter values affecting the performance characteristics by designing the STHE. During this step, layout of the tubes, number of baffles, number of tubes, length, the distance between baffles, and cross section of the baffle are defined. In the parameter design step, the best level of parameters are defined to optimize the heat exchanger. At this stage, factors that reduce

Table 1
Properties of the fluids in the heat exchanger.

Parameter	Hot Water (Tube side)		Cold Water (Shell side)	
Mean fluid temperature (K)	338	346	294	298
Mass flow rates (kg/s)	0.50	2.88	0.20	2.19
Density (kg/m^3)	980.4	977.52	998.0	997.0
Specific heat (kJ/kg.K)	4.187	4.191	4.182	4.180
Thermal conductivity (W/m.K)	0.659	0.665	0.598	0.607
Kinematic viscosity (m^2/s)	0.444×10^{-6}	0.399×10^{-6}	1.004×10^{-6}	0.894×10^{-6}
Prandtl Number	2.75	2.30	7.01	6.14

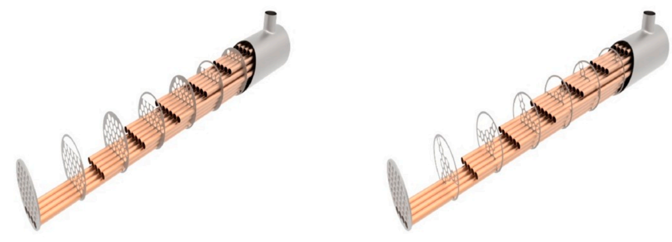

(a) Conventional baffle (b) Three-zonal baffle

Fig. 1. The heat exchangers with conventional and three-zonal baffles.

pressure drop and increase heat transfer are determined and the orthogonal arrays developed by Taguchi are used while blocking the parameters. At the same time, the noise ratio (S/N - Signal/Noise) analyses are performed. There are three different convenient functions known as Taguchi loss function and also expressed as a function of noise ratio (S/N, Signal/Noise). These are cases where the performance characteristic is called the least favorable result;

$$S \Big/ N = -10\log\left(\frac{1}{n}\sum_{i=1}^{n} {y_i}^2\right) \tag{1}$$

In the case of the highest value is the best:

$$S \Big/ N = -10\log\left(\frac{1}{n}\sum_{i=1}^{n} \frac{1}{{y_i}^2}\right) \tag{2}$$

When the nominal value is the best:

$$S \Big/ N = 10\log\left(\frac{\overline{y}^2}{S^2}\right) \tag{3}$$

where $\overline{y} = \frac{1}{n}\sum_{i=1}^{n} y_i$, $S^2 = \frac{1}{n-1}\sum_{i=1}^{n}(y_i - \overline{y})^2$, y_i is the performance characteristic of performance, n is number of test in trial, $\overline{y}$ is average of observed values, and S^2 is the variance of observation value.

In this study, the three-zonal baffle was optimized to provide the maximum heat transfer rate and the minimum pressure drop. While designing the geometry of the three-zonal baffle, five factors, and four levels of these factors were considered. Table 3 gives these factors and corresponding levels. Cross-sectional view of the three-zonal baffle is shown in Fig. 5.

When these factors and their levels were taken into consideration, it was decided that the most appropriate orthogonal array was L_{16} sequence. The order of the experiments according to this orthogonal array is shown in Table 4.

4. Experimental studies

4.1. Experimental setup and test procedure

The experimental studies were carried out on a STHE which has the geometric dimensions obtained from the optimization. The tube-side flow was supported by a frequency converter pump with a closed loop. The hot water tank was heated by electrical heaters in order to keep the temperature constant. A continuous stirrer helped to maintain the liquid temperature at a constant value for a given test flow rate. On the other hand, the cold water was controlled with the frequency converter pump and the heated water was evacuated out in a tank. Flow and temperature control were done at the heat exchanger inlet and outlet points. The experimental setup is shown in Fig. 6. During the experiments, flow rate and temperature control were done with the control panel and necessary controls were provided.

The basic elements used in the experimental setup are hot and cold water tanks, STHE and control panel. The system also includes globe

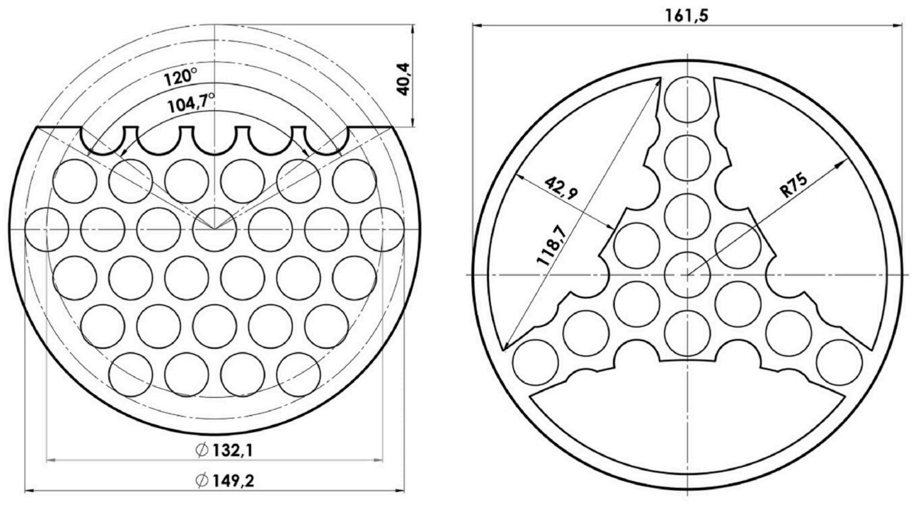

(a) Conventional baffle (b) Three-zonal baffle

Fig. 2. Geometric dimensions of the conventional and three-zonal baffles.

Table 2
Specifications of the heat exchanger.

Shell diameter	161.5 mm
Tube outlet diameter	17.2 mm
Tube layout and distance between the tubes	Triangle, 22 mm
Number of tubes	37
Heat exchanger length	1356.5 mm
Central baffle distance	193.5 mm
Number of baffle	6
Tube-to-baffle clearance	0.4
Shell-to-baffle clearance	0
Shell-to-bundle clearance	12.3

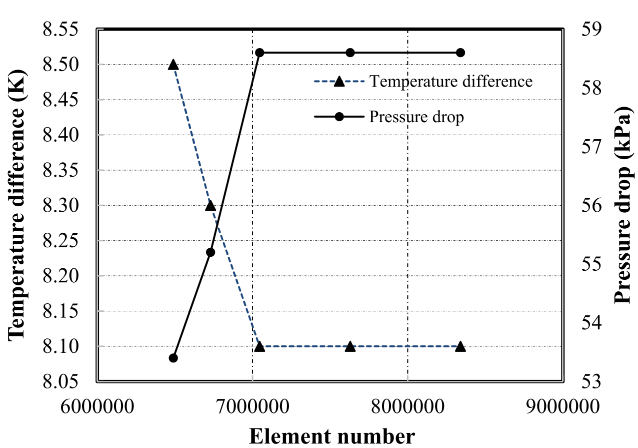

Fig. 3. Element number independency of the numerical solution.

valves, manometers to measure the pressure differences of the fluids entering and exiting the heat exchanger, and PT100 thermocouples for measuring the temperature of the hot and cold fluids, and two pumps to circulate two streams. Before getting the experimental data, the valve in the tube from which the water came from was opened and the system was expected to be filled completely. Then the cold water outlet valve was opened and the control panel provided hot and cold pumping at the desired flow rate. After a certain period of time, the system became stable and the necessary measurement results were taken.

Experiments were performed for seven different input conditions. When the heater capacities were 15 kW, the analyses were performed for low flow rates to ensure the stability of the temperature. Table 5 presents the conditions for hot and cold fluids entering the heat exchanger. Heat transfer rate was calculated by using the following equation;

$$\dot{Q} = \dot{m} c_p \Delta T \tag{4}$$

where, $\dot{Q}$ is heat transfer rate, $\dot{m}$ is mass flow rate, c_p is specific heat of the fluid, and ΔT is temperature difference.

4.2. Uncertainty analysis

The measuring process of parameters such as mass flow rate and temperature always have some errors and these lead to an uncertainty in experimental data. The thermocouples and flow meter outputs are used to calculate experimental heat transfer rate. In this study, experimental uncertainties were calculated by Holman [47] method. The following equations were used to calculate the uncertainty. The uncertainty is consists of two parts: the uncertainty of instruments ($u_{\dot{Q},Ins}$) and the uncertainty of repeatability ($u_{\dot{Q},Rep}$).

$$U_{\dot{Q}} = K \times u_{\dot{Q}} \tag{5}$$

$$u_{\dot{Q}=}\sqrt{\left(u_{\dot{Q},Ins}\right)^2 + \left(u_{\dot{Q},Rep}\right)^2} \tag{6}$$

$$u_{\dot{Q},\ Ins} = \sqrt{\left(\frac{\partial \dot{Q}}{\partial \dot{m}} u_{\dot{m}}\right)^2 + \left(\frac{\partial \dot{Q}}{\partial \Delta T} u_{\Delta T}\right)^2} \tag{7}$$

$$u_{\dot{Q},\ Rep} = \sqrt{\left(\frac{\partial \dot{Q}}{\partial \dot{m}} u_{\dot{m}}\right)^2 + \left(\frac{\partial \dot{Q}}{\partial \Delta T} u_{\Delta T}\right)^2} \tag{8}$$

where $u_{\dot{Q},Ins}$ is the uncertainty of instruments, $u_{\dot{Q},Rep}$ is the uncertainty of repeatability, u is the contribution of the uncertainty in the results from parameters $\dot{m}$ and ΔT, K is the coverage factor and was considered as 2 in this case. Table 6 shows the measurement ranges, measurement accuracy of the measuring devices used in the experimental setup, and uncertainty levels of the calculated parameters based on experimental data.

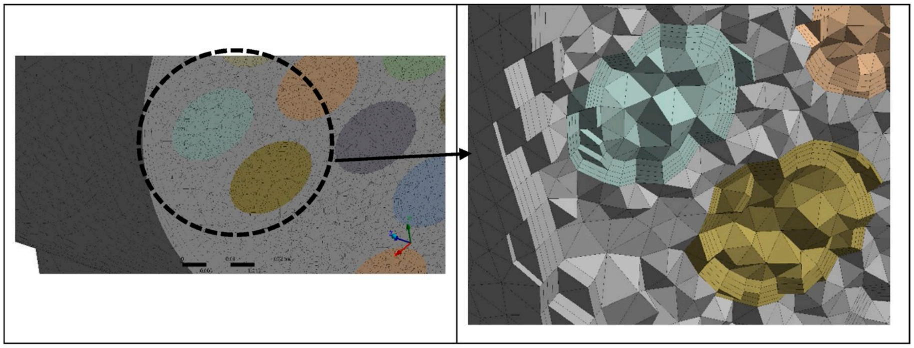

Fig. 4. General view of the mesh structure.

Table 3
The design factors and their levels.

Parameters	Level 1	2	3	4
A: Distance between baffles (mm)	250	316	400	420
B: Rotation angle of the baffle (degree)	0	60	120	180
C: The ratio of outer diameter to inner diameter (D_o/D_i)	1.15	1.11	1.08	1.04
D: Angle of openness to center (degree)	100	103	105	106
E: The ratio of openness to closure (S_o/S_c)	2.52	2.85	3.36	4.11

5. Results and discussion

In this study, CFD analyzes were performed in two different mass flow rates. One of these mass flow rates was determined as low mass flow rate (0.5 kg/s), and the other as high mass flow rate (2.88 kg/s). In Figs. 7–9, temperature, pressure, and velocity distributions obtained from CFD analyses for mass flow rate of 0.5 kg/h were given. On the other hand, the numerical results obtained from the CFD analyses for both mass flow rates were presented and compared In Table 7.

5.1. Results of the CFD analyses

Fig. 7 shows the temperature distributions on tube surfaces in heat exchangers having conventional and three-zonal baffles. As can be seen from the figures, when the three-zonal baffles are used, a much more uniform temperature distribution is obtained on the tube surfaces compared to the conventional baffle. In the figure, the temperatures at two same selected points on tube surfaces were also shown for both heat exchangers. The tube surface temperatures at these two points were 334 °C in the conventional heat exchanger, and 328 °C in the heat exchanger with three-zonal baffle. This indicate that a better heat transfer from the hot fluid to the cold fluid is achieved in the heat exchanger with the use of a three-zonal baffle.

Fig. 8 shows the pressure distributions on heat exchangers having conventional and three-zonal baffles. The figures show that the three-zonal baffles give a much more uniform pressure distribution compared to the conventional baffle. It is seen from the figure that when three-zonal baffles are used, pressures decreases dramatically compared to conventional baffles.

Fig. 9 shows velocity streamlines in heat exchangers with conventional and three-zonal baffle. As can be seen from the figures, in the heat exchanger having conventional baffles, recirculation zones are formed at the rear of the baffles. In the conventional baffle, the fluid is forced to change direction at an angle of about 90° in front of each baffle on the shell side. The purpose of this is to forward the flow streams on the shell side perpendicular onto the tube bundle in order to maximize the forced convective heat transfer coefficient. This increases the heat transfer coefficient by a certain amount, but also leads to large pressure drop, causes the formation of recirculation zones at the junction of the baffle

Table 4
The order of experiments according to the orthogonal array.

Experiment number	A	B	C	D	E
1	1	1	1	1	1
2	1	2	2	2	2
3	1	3	3	3	3
4	1	4	4	4	4
5	2	1	2	3	4
6	2	2	1	4	3
7	2	3	4	1	2
8	2	4	3	2	1
9	3	1	3	4	2
10	3	2	4	3	1
11	3	3	1	2	4
12	3	4	2	1	3
13	4	1	4	2	3
14	4	2	3	1	4
15	4	3	2	4	1
16	4	4	1	3	2

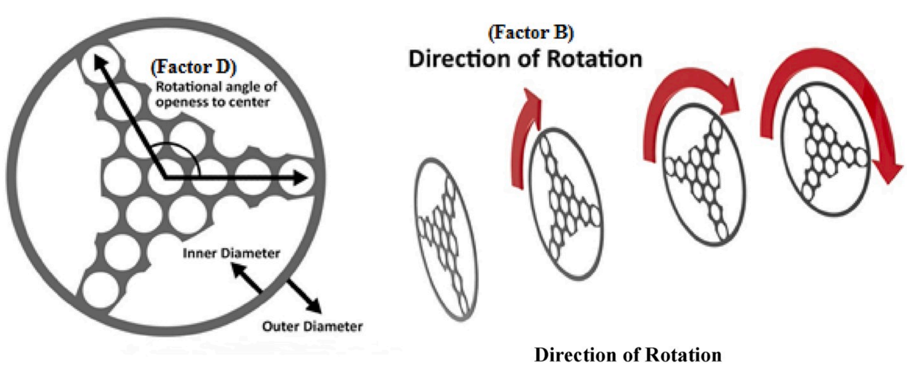

Fig. 5. Cross-sectional view of the three-zonal baffle.

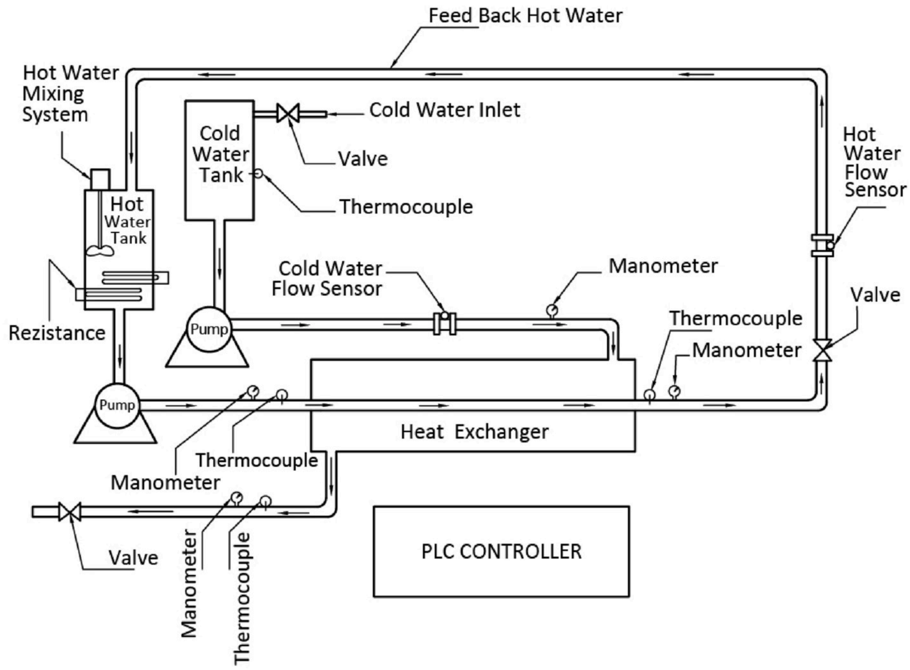

Fig. 6. Experimental setup.

Table 5
Heat exchanger input parameters.

Tube-Side		Shell-Side	
Mass flow rate (kg/s)	Inlet temperature (K)	Mass flow rate (kg/s)	Inlet temperature (K)
0.3	323	0.3	295
0.4	323	0.4	295
0.5	323	0.5	295
0.6	323	0.6	295
0.7	323	0.7	295
1.0	323	0.8	295
2.1	323	1.0	295

Table 6
Measuring ranges and measurement accuracy of the devices used in the experiments and uncertainty levels of the calculated parameters.

Equipment	Range	Accuracy	Uncertainty (%)
PT100	0/100 °C	±1 °C	
Manometer	0/100 mbar	2 mbar	
	0/2.5 bar	0.02 bar	
Flow meter	0/50 l/s	0.01 l/s	
Heat transfer rate	–	–	1.5

and the shell, and consequently worsens the heat transfer in these zones. The recirculation zones are also susceptible to fouling. These recirculation zones reduce the heat transfer from the hot fluid to the cold fluid on the one hand, while increasing the fouling resistance in these areas. Increased fouling resistance reduces the service life of the heat exchanger, increases the operating and maintenance costs of the heat exchanger. In addition, the heat transfer in these recirculation zones decreases depending on time and the efficiency of the heat exchanger is reduced. In the case of three-zonal baffle, these recirculation zones are almost never formed. With the new baffle design, these recirculation zones are substantially eliminated and the average flow velocity on the tube bundle is maintained substantially. As a result, the effective heat transfer surface area is increased, and an effective mixture on the shell side is obtained. This also improves the heat transfer mechanism.

Table 7 compares the temperature difference and pressure drops that occur in heat exchangers with conventional and three-zonal baffles under different operating conditions. As seen from the table, at the conditions of 0.5 kg/s hot water mass flow rate and 0.2 kg/s cold water mass flow rate, the temperature difference for conventional and three-zonal baffles were obtained as 44.3 K, and 47.3 K, respectively. On the other hand, for the mass flow rates of 2.19 kg/s and 2.88 kg/s, a temperature difference of 16.3 K in the conventional heat exchanger, and 17.4 K in the heat exchanger with three-zonal baffle were obtained. These results show that the temperature difference in the heat exchanger increases with decreasing mass flow rates and the maximum increase up to 6.75% with the use of three-zonal baffles.

It is seen from the table that the three-zonal baffle heat exchanger gives much better results in terms of pressure drop compared to conventional heat exchanger. According to the CFD analyses results, the pressure drop in the heat exchanger was 79.9 Pa in the case of conventional baffle and 51.8 Pa in the case of three-zonal baffle at the lower mass flow rate condition. As the mass flow rate increases, the decrease in the pressure drop in the heat exchange with three-zonal baffle becomes much more pronounced. At the higher mass flow rate conditions, the pressure drop in the heat exchanger was obtained as 9431.2 Pa in the case of conventional baffle and 4836.7 Pa in the case of three-zonal baffle. The maximum reduction in pressure drop has increased up to 49%. These results show that the thermal performance of the heat exchanger can be improved as well as the pressure drop can be dramatically reduced with the use of the newly designed three-zonal baffles. In Table 7, the pressure drop values calculated by using the Kern method for the conventional heat exchanger were also presented to validate the CFD analyses results. The results show that there is a difference of up to 16% between the pressure drop values calculated by the Kern method and the CFD analyses results.

Similar results were obtained in an experimental study conducted by Yang et al. [14]. Their experimental results showed that the use of unilateral ladder type helical baffle resulted in a 15.3–47.1% reduction in pressure drop and an increase in shell side heat transfer coefficient of 9.3–25.5% compared to segmental baffle use. Dandgaval et al. [19], numerically investigated the effects of helical and two different segmental baffles usage on the shell and tube heat exchanger performance. They stated that the use of helical baffle prevented the formation

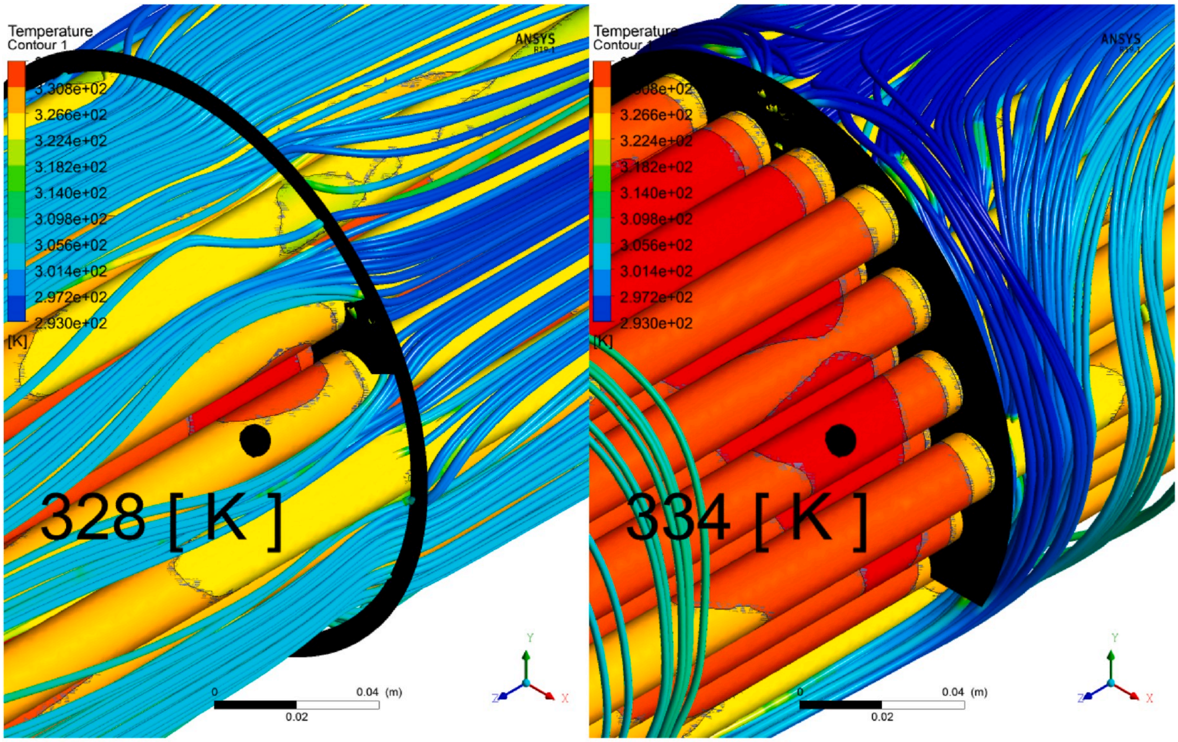

(a) Three-zonal baffle **(b) Conventional baffle**

Fig. 7. Temperature distributions in the heat exchanger at a mass flow rate of 0.5 kg/s.

of dead zones behind the baffle, thereby pressure drop was decreased, and thermal performance was improved. Chen et al. [21] investigated the effects of different helical baffle designs on pressure drop and thermal performance of the heat exchanger. Their numerical results indicated that the helical baffle reduced the pressure drop, and improved thermal performance compared to the segmental baffle. However, the main improvement here is not to increase the rate of heat transfer, but to lower the pressure drop in the shell side without worsening the heat transfer. This result was obtained by providing a more intense and homogeneous mixing on the shell side and eliminating the recirculation zones and stagnation points. Both CFD results and experimental measurements confirm this conclusion.

5.2. Taguchi optimization results

Table 8 shows the CFD results of the cold water outlet temperature and pressure drop values in the heat exchanger, which was carried out by taking the experimental conditions determined according to Taguchi optimization method. The results of the analyses show that the maximum outlet temperature is obtained under test conditions 1 and the minimum pressure drop value is obtained under test conditions 13.

Optimum conditions were determined by using Taguchi method for cold water outlet temperature. As the generated design has not been included in the main experimental layout, the process was re-iterated until the required criteria are satisfied. Fig. 10 shows the Taguchi analyses results performed with Minitab statistical software for cold water outlet temperature. After confirmation test carried out at the 99% confidence level, the optimum design factor combination of the baffle were obtained by taking into account level 1 of factor A, level 3 of factor B, level 1 of factor C, level 1 of factor D, and level 1 of factor E (A1B3C1D1E1). Since this experiment was not included among the defined 16 experiments, the outlet temperature was estimated as 331.5 K considering optimized factors.

The second objective was to minimize the pressure drop in the heat exchanger. The results of Taguchi analyses performed for this purpose are shown in Fig. 11. As can be seen in the figure, level 4 of factor A, level 2 of factor B, level 4 of factor C, level 2 of factor D and level 4 of factor E should be considered to minimize the pressure drop (A4B2C4D2E4). Since there is no defined experiment with these levels of factors among the 16 designed experiments, CFD analyses considering the optimized factor values was carried out and the pressure drop was obtained as 26.5 Pa.

The confirmation tests were performed and the results were presented in Table 9 and Table 10. In Table 9, predicted and actual cold water outlet temperature are presented. As can be seen from the table, there is very good agreement between predicted and actual values. The results show that improvement in S/N ratio for cold water outlet temperature is 0.013 dB. The cold water outlet temperature was also approximately 0.15% increased. On the other hand, Table 10 shows predicted and actual pressure drop values. For pressure drop, the improvement in S/N ratio was 4.3 dB, and the decrease in pressure drop was approximately 39.27%. The results obtained from confirmation tests confirmed the validity of the Taguchi approach used in the optimization of design parameters.

Table 11 shows ANOVA variance analyses results. As can be seen from the table, the most important design factor in terms of temperature is A with at least 99.99% confidence level. Factors C and D are less effective. On the other hand, factors B and E are significant but not effective. In terms of pressure drop, the most important design factors are A, C and E with a confidence level of 95%. However, factors B and D are less effective.

5.3. Validation of CFD results

In the study, the CFD analyses results were validated with the experimental data. For this purpose, the heat exchanger with conventional and three-zonal baffles were tested for seven non-consecutive different mass flow rates and the results were used to validate the CFD analyses results performed under the same operating conditions. In Figs. 12 and 13, this validation is performed in terms of pressure drop

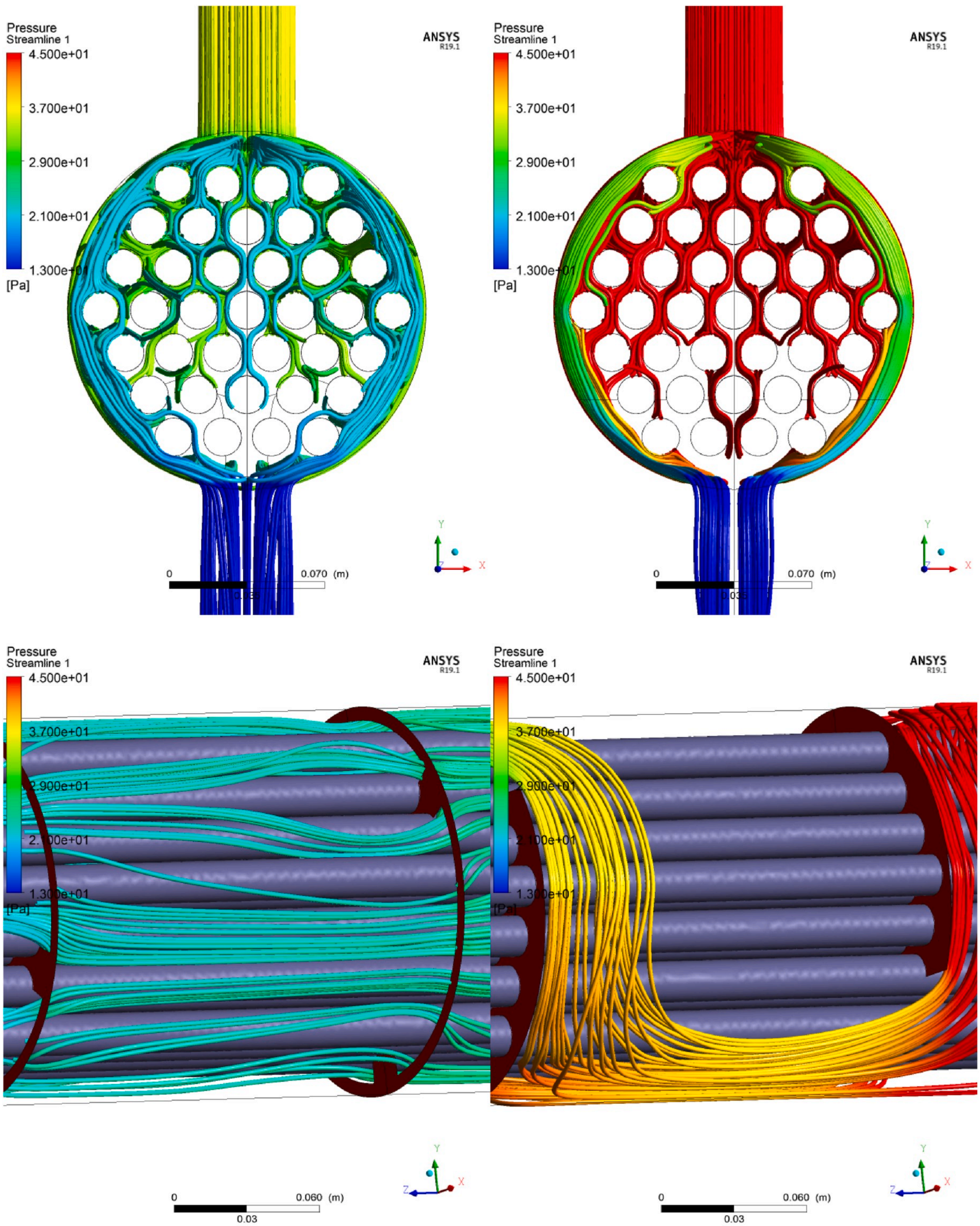

(a) Three-zonal baffle **(b) Conventional baffle**

Fig. 8. Pressure distributions in the heat exchanger at a mass flow rate of 0.5 kg/s.

and heat transfer rate, respectively. The results show a good agreement between the CFD analyses results and the experimental values.

In Fig. 12, the tube-side experimental pressure drops are compared with the calculated pressure drops based on CFD analyses for the three-zonal baffle. As can be seen from the figure, the pressure drop in the tubes increase with the increase of the mass flow rate as expected. The experimental pressure drops were calculated in the range of 23.5–240 Pa, and the pressure drops calculated based on CFD analyses were in the range of 25.3–257.1 Pa. There was a difference up to 7.6% between the experimental values and the CFD results.

The heat transfer rates of the heat exchangers calculated using the experimental and CFD data are compared in Fig. 13. The horizontal axis in the figure shows seven non-consecutive mass flow rate values for which experiments and analyzes were performed. As shown in the figure, the heat transfer rate increases as the mass flow rate increases for both baffles. A difference of up to 7.3% occurred between the

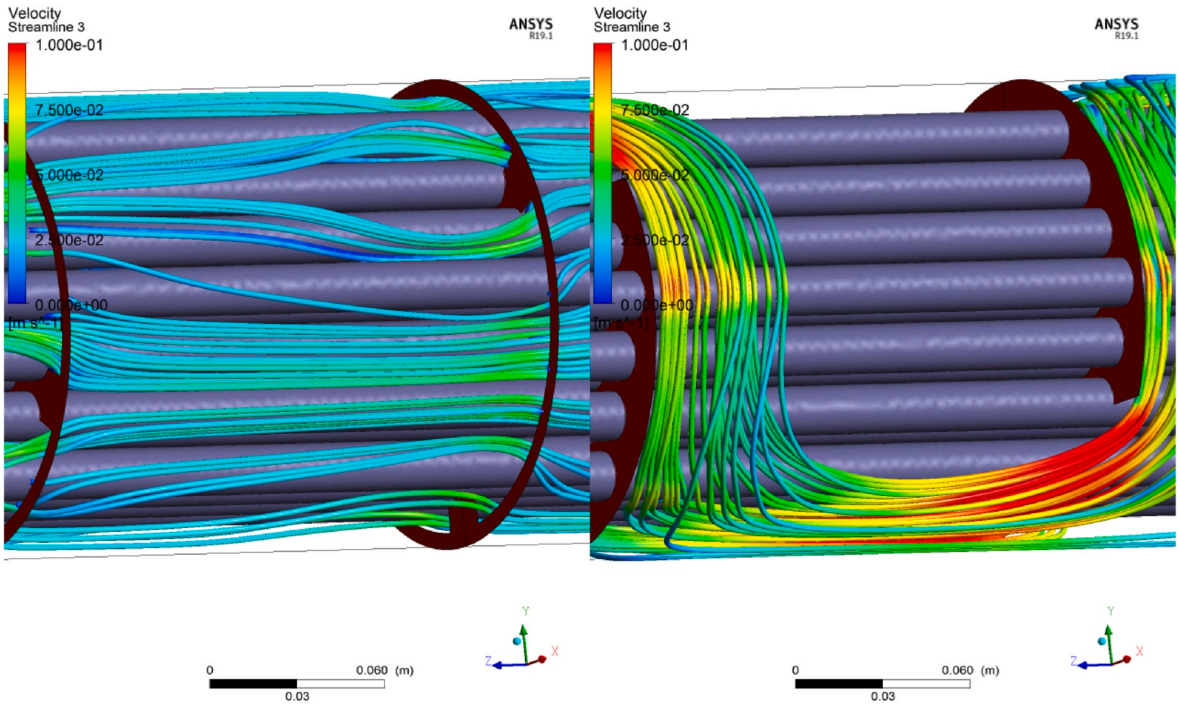

(b) Three-zonal baffle (b) Conventional baffle

Fig. 9. Velocity streamlines in the heat exchanger at a mass flow rate of 0.5 kg/s.

Table 7
Temperature difference and pressure drops in heat exchangers with conventional and three-zonal baffles.

Baffle type	Mass flow rate of cold water (kg/s)	Mass flow rate of hot water (kg/s)	Temperature difference between inlet and outlet (K) (CFD)	Pressure drop (Pa) (CFD)	Pressure drop (Pa) (Kern)
Three-zonal	2.19	2.88	17.4	4836.7	–
Conventional	2.19	2.88	16.3	9431.2	10693.4
Three-zonal	0.2	0.5	47.3	51.8	–
Conventional	0.2	0.5	44.3	79.9	93.4

Table 8
Pressure and temperature values obtained by CFD analyses.

Experiment number	A	B	C	D	E	Temperature (K)	Pressure (Pa)
1	1	1	1	1	1	331.3	43.14
2	1	2	2	2	2	328.7	32.43
3	1	3	3	3	3	330.1	32.18
4	1	4	4	4	4	328.1	31.77
5	2	1	2	3	4	325.3	38.21
6	2	2	1	4	3	325.7	37.96
7	2	3	4	1	2	325.8	33.05
8	2	4	3	2	1	325.8	37.81
9	3	1	3	4	2	326.1	32.81
10	3	2	4	3	1	326.1	32.61
11	3	3	1	2	4	326.7	32.54
12	3	4	2	1	3	327.4	32.63
13	4	1	4	2	3	327.7	29.96
14	4	2	3	1	4	328.6	30.09
15	4	3	2	4	1	328.4	35.31
16	4	4	1	3	2	329.7	34.01

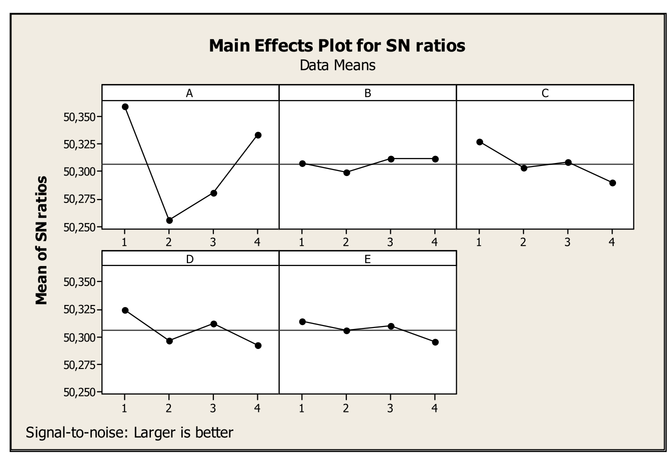

Fig. 10. Taguchi analyses results performed with Minitab statistical software for cold water outlet temperature.

experimental values and the CFD results.

6. Conclusions

In this study, a new three-zonal baffle was designed for use in the STHEs. After that, CFD analyzes of the heat exchangers with conventional and three-zonal baffles were performed and the results of the analyses were compared. The shell-and-tube heat exchanger with the newly developed three-zonal baffle was then optimized using the Taguchi method. In the final stage of the study, the results of CFD analyses using optimized baffles were validated with the experimental results obtained under the same working conditions. The conclusions obtained in this study are as follows:

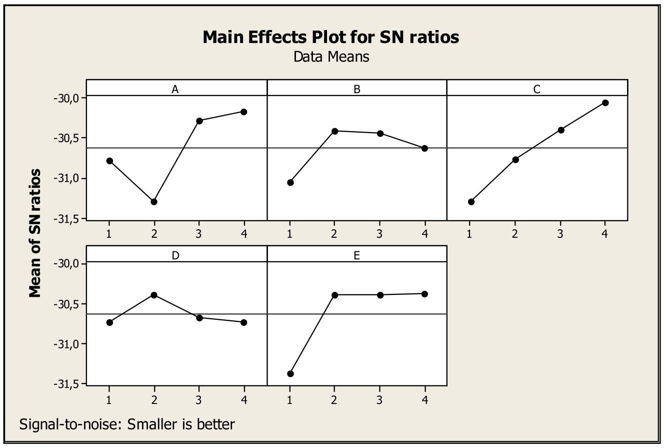

Fig. 11. Taguchi analyses results performed with Minitab statistical software for pressure drop.

Table 9
Confirmation test results for cold water outlet temperature.

	Initial parameters	Optimum parameters	
		Prediction	Experiment
Level	A1B1C1D1E1	A1B3C1D1E1	A1B3C1D1E1
Temperature	331.3	331.5	331.8
S/N ratio (dB)	50.404	50.409	50.417

Table 10
Confirmation test results for pressure drop.

	Initial parameters	Optimum parameters	
		Prediction	Experiment
Level	A1B1C1D1E1	A4B2C4D2E4	A4B2C4D2E4
Pressure drop	43.14	26.50	26.20
S/N ratio (dB)	−32.70	−28.50	−28.40

Table 11
The variance analysis (ANOVA).

	Factors	Sum of Squares, SS	Degree of Freedom v	Variance, V	F_{factor}
Temperature	A	0.0271	3	0.0090	16.28[b]
	B	0.0004	3	0.0001	0.25
	C	0.0029	3	0.0010	1.74
	D	0.0025	3	0.0008	1.52
	E	0.0008	3	0.0003	0.39
	Total	0.0338	15	0.0023	
	ep	0.0067	12.00	0.0006	
Pressure drop	A	3.1728	3	1.0576	9.91[a]
	B	1.0438	3	0.3479	3.26
	C	3.3662	3	1.1221	10.52[a]
	D	0.3201	3	0.1067	1.00
	E	2.9147	3	0.9716	9.10[a]
	Total	10.82	15	1.06	
	ep	0.32	3.00	0.11	

[a] At Least 95% confidence.
[b] At Least 99.99% confidence.

- The three-zonal baffle does not partially block the flow in the shell-side. Thus, there are no stagnant zones behind the baffles. This reduces the fouling and ensures long-term operating periods.
- In the case of using three-zonal baffles, very low pressure drops in the shell-side occur compared to conventional baffles. With the use of three-zonal baffles, to the pressure loss in the shell-side has lowered by 49% compared to conventional segmentally baffled configuration. Thus, it will be possible to reduce operating costs by using a pump with lower input power.

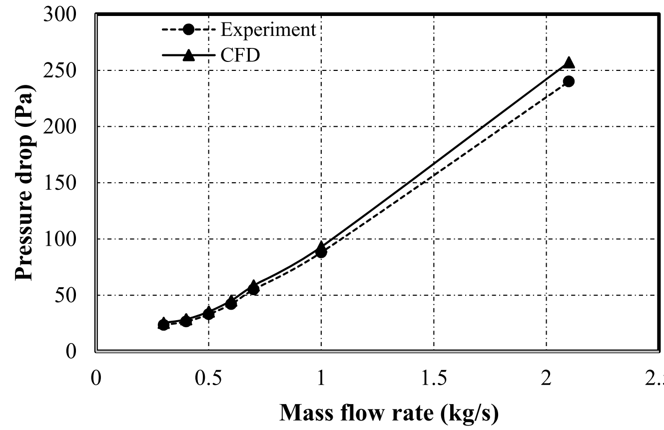

Fig. 12. Pressure difference on the tube side of the heat exchanger.

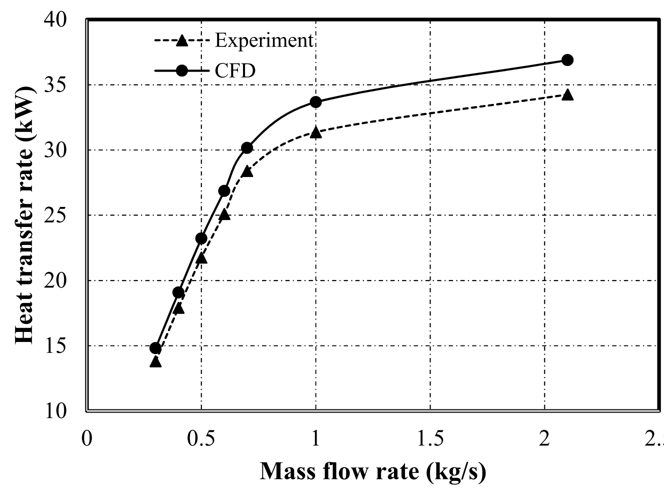

Fig. 13. Tube side heat transfer rate of the heat exchanger.

- The use of a three-zonal baffle has resulted in significant increases in temperature differences in the heat exchanger compared to conventional baffles. The maximum increase was obtained as 6.75% depending on the operating conditions of the heat exchanger. This means that the thermal capacity of the heat exchanger will increase with the use of a three-zonal baffle, and that the same thermal performance can be achieved with a more compact heat exchanger.
- The flow induced vibration in the shell-side of the heat exchanger could be considerably reduced with the use of new three-zonal baffles.

Declaration of competing interest

The authors declare that they have no known competing financial interests or personal relationships that could have appeared to influence the work reported in this paper.

References

[1] S. Kakac, H. Liu, A. Pramuanjaroenkij, Heat Exchangers Selection, Rating and Thermal Design, third ed., CRC Press, Washington D.C., 2012.
[2] M. Petrik, G.L. Szepesi, Shell side CFD analysis of a model shell-and-tube heat, Chemıcal Engıneerıng Transactıons 70 (2018) 313–318.
[3] C. Yua, T. Chengb, J. Chenb, Z. Renb, M. Zeng, Investigation on thermal-hydraulic performance of parallel-flow shell and tube heat exchanger with a new type of anti-vibration baffle and wire coil using RSM method, Int. J. Therm. Sci. 138 (2019) 351–366.

[4] B.I. Master, K.S. Chunangad, A.J. Boxma, D. Kral, P. Stehlík, Most frequently used heat exchangers from pioneering research to worldwide applications, Heat Tran. Eng. 27 (2006) 4–11.
[5] L. Liebenberg, J.P. Meyer, In-tube passive heat transfer enhancement in the process industry, Appl. Therm. Eng. 27 (2007) 2713–2726.
[6] S. Yang, Y. Chen, J. Wu, H. Gu, Influence of baffle configurations on flow and heat transfer characteristics of unilateral type helical baffle heat exchangers, Appl. Therm. Eng. 133 (2018) 739–748.
[7] S.K. Singh, D. Stephan, in: https://www.process-worldwide.com/, 2014.
[8] J. Mahendran, Experimental analysis of shell and tube heat exchanger using flower baffle plate configuration, Materials Today:Proceedings 21 (2020) 419–424.
[9] K. Wang, C. Bai, Y. Wang, M. Liu, Flow dead zone analysis and structure optimization for the trefoil-baffle heat Exchanger, Int. J. Therm. Sci. 140 (2019) 127–134.
[10] L. Ma, K. Wang, M. Liu, D. Wang, T. Liu, Y. Wang, Z. Liu, Numerical study on performances of shell-side in trefoil-hole and quatrefoil-hole baffle heat exchangers, Appl. Therm. Eng. 123 (2017) 1444–1455.
[11] C. Donga, X.F. Zhoub, R. Dongc, Y.Q. Zhenga, Y.P. Chend, G.L. Hua, Y.S. Xua, Z. G. Zhanga, W.W. Guo, An analysis of performance on trisection helical baffles heat exchangers with diverse inclination angles and baffle structures, Chem. Eng. Res. Des. 121 (2017) 421–430.
[12] X. Cao, T. Du, Z. Liu, H. Zhai, Z. Duan, Experimental and numerical investigation on heat transfer and fluid flow performance of sextant helical baffle heat exchangers, Int. J. Heat Mass Tran. 142 (2019) 118437.
[13] J. Chen, X. Lu, Q. Wang, M. Zeng, Experimental investigation on thermal-hydraulic performance of a novel shell-and-tube heat exchanger with unilateral ladder type helical baffles, Appl. Therm. Eng. 161 (2019) 114099.
[14] S. Yang, Y. Chen, J. Wu, H. Gu, Influence of baffle configurations on flow and heat transfer characteristics of unilateral type helical baffle heat exchangers, Appl. Therm. Eng. 133 (2018) 739–748.
[15] S. Shinde, U. Chavan, Numerical and experimental analysis on shell side thermo-hydraulic performance of shell and tube heat exchanger with continuous helical FRP baffles, Thermal Science and Engineering Progress 5 (2018) 158–171.
[16] L. He, P. Li, Numerical investigation on double tube-pass shell-and-tube heat exchangers with different baffle configurations, Appl. Therm. Eng. 143 (2018) 561–569.
[17] T. Dua, Q. Chen, W. Dua, L. Cheng, Performance of continuous helical baffled heat exchanger with varying elliptical tube layouts, Int. J. Heat Mass Tran. 133 (2019) 1165–1175.
[18] S. Yang, Y. Chen, J. Wu, H. Gu, Performance simulation on unilateral ladder type helical baffle heat exchanger in half cylindrical space, Energy Convers. Manag. 150 (2017) 134–147.
[19] B.O. Dandgaval, P.D.R. Godase, T. Dey, Study of shell and tube heat exchanger with the effect of types of baffles, Procedia Manufacturing 20 (2018) 195–200.
[20] G. Yang, G. Ding, J. Chen, W. Yang, S. Hu, Experimental study on shell side heat transfer characteristics of two-phase propane flow condensation for vertical helically baffled shell-and-tube exchanger, Int. J. Refrig. 107 (2019) 135–144.
[21] Y. Chen, H. Tang, J. Wu, H. Gu, S. Yang, Performance comparison of heat exchangers using sextant/trisection helical baffles and segmental ones, Chin. J. Chem. Eng. 12 (2019) 2892–2899.
[22] M. Miansari, A. Jafarzadeh, H. Arasteh, D. Toghraie, Thermal performance of a helical shell and tube heat exchanger without fin, with circular fins, and with V-shaped circular fins applying on the coil, J. Therm. Anal. Calorim. (2020). In press, corrected proof, Available online 07 February 2020.
[23] E.M.S. El-Saida, M.M.A. Al-Sood, Shell and tube heat exchanger with new segmental baffles configurations: a comparative experimental investigation, Appl. Therm. Eng. 150 (2019) 803–810.
[24] J. Chen, P. Zhao, Q. Wang, M. Zeng, Experimental investigation of shell-side performance and optimal design of shell-and-tube heat exchanger with different flower baffles, Heat Tran. Eng. (2020). In press, corrected proof, Available online 04 February 2020.
[25] X. Wang, N. Zheng, Z. Liu, W. Liu, Numerical analysis and optimization study on shell-side performances of a shell and tube heat exchanger with staggered baffles, Int. J. Heat Mass Tran. 124 (2018) 247–259.
[26] X. Gu, Y. Luo, X. Xiong, K. Wang, Y. Wang, Numerical and experimental investigation of the heat exchanger with trapezoidal baffle, Int. J. Heat Mass Tran. 127 (2018) 598–606.
[27] J. Xiao, S. Wang, S. Ye, J. Wang, J. Wen, J. Tu, Experimental investigation on pre-heating technology of coal water slurry with different concentration in shell-and-tube heat exchangers with ladder-type fold baffles, Int. J. Heat Mass Tran. 132 (2019) 1116–1125.
[28] C. Yu, Z. Ren, M. Zeng, Numerical investigation of shell-side performance for shell and tube heat exchangers with two different clamping type anti-vibration baffles, Appl. Therm. Eng. 133 (2018) 125–136.
[29] C. Yua, J. Chenb, M. Zengb, B. Gao, Numerical study on turbulent heat transfer performance of a new parallel flow shell and tube heat exchanger with sinusoidal wavy tapes using RSM analysis, Appl. Therm. Eng. 150 (2019) 875–887.
[30] X. Wang, Y. Liang, Y. Sun, Z. Liu, W. Liu, Experimental and numerical investigation on shell-side performance of a double shell-pass rod baffle heat exchanger, Int. J. Heat Mass Tran. 132 (2019) 631–642.
[31] Y. Lei, Y. Li, S. Jing, C. Song, Y. Lyu, F. Wang, Design and performance analysis of the novel shell-and-tube heat exchangers with louver baffles, Appl. Therm. Eng. 125 (2017) 870–879.
[32] G.B. Leoni, T.S. Klein, R.A. Medronho, Assessment with computational fluid dynamics of the effects of baffle clearances on the shell side flow in a shell and tube heat exchanger, Appl. Therm. Eng. 112 (2017) 497–506.
[33] M. Mellal, R. Benzeguir, D. Sahel, H. Ameur, Hydro-thermal shell-side performance evaluation of a shell and tube heat exchanger under different baffle arrangement and orientation, Int. J. Therm. Sci. 121 (2017) 138–149.
[34] A.A.A. Arania, R. Moradi, Shell and tube heat exchanger optimization using new baffle and tube configuration, Appl. Therm. Eng. 157 (2019) 113736.
[35] C.S. Pandey, H. Sharma, M. Dadhich, S.K. Jain, Numerical analysis and optimization of corrugated heat exchanger with Taguchi method, Int. J. Res. Appl. Sci. Eng. Technol. 6 (2018) 874–879.
[36] S. Gunes, E. Manay, E. Senyigit, V. Ozceyhan, A Taguchi approach for optimization of design parameters in a tube with coiled wire inserts, Appl. Therm. Eng. 31 (2011) 2568–2577.
[37] S. Chamoli, A Taguchi approach for optimization of flow and geometrical parameters in a rectangular channel roughened with V down perforated baffles, Case Stud., *Therm. Eng.* 5 (2015) 59–69.
[38] L.H. Tang, S.C. Tan, P.Z. Gao, M. Zeng, Parameters optimization of fin-and tube heat exchanger with a novel vortex generator fin by Taguchi method, Heat Tran. Eng. 37 (2016) 369–381.
[39] M. Zeng, L.H. Tang, M. Lin, Q.W. Wang, Optimization of heat exchangers with vortex-generator fin by Taguchi method, Appl. Therm. Eng. 30 (2010) 1775–1783.
[40] A.Z. Aghaie, A.B. Rahimi, A. Akbarzadeh, A general optimized geometry of angled ribs for enhancing the thermo-hydraulic behavior of a solar air heater channel – a Taguchi approach, Renew. Energy 83 (2015) 47–54.
[41] T. Du, W. Du, K. Che, L. Cheng, Parametric optimization of overlapped helical baffled heat exchangers by Taguchi method, Appl. Therm. Eng. 85 (2015) 334–339.
[42] T. Sivasakthivel, K. Murugesan, H.R. Thoma, Optimization of operating parameters of ground source heat pump system for space heating and cooling by Taguchi method and utility concept, Appl. Energy 116 (2014) 76–85.
[43] M.M. Etghani, S.A.H. Baboli, Numerical investigation and optimization of heat transfer and exergy loss in shell and helical tube heat exchanger, Appl. Therm. Eng. 121 (2017) 294–301.
[44] J.N. Zhang, M. Cheng, Y.D. Ding, Q. Fu, Z.Y. Chen, Influence of geometric parameters on the gas-side heat transfer and pressure drop characteristics of three-dimensional finned tube, Int. J. Heat Mass Tran. 133 (2019) 192–202.
[45] S. Chamoli, P. Yu, A. Kumar, Multi-response optimization of geometric and flow parameters in a heat exchanger tube with perforated disk inserts by Taguchi grey relational analysis, Appl. Therm. Eng. 103 (2016) 1339–1350.
[46] M. Miansari, M.A. Valipour, H. Arasteh, D. Toghraie, Energy and exergy analysis and optimization of helically grooved shell and tube heat exchangers by using Taguchi experimental design, J. Therm. Anal. Calorim. 139 (2020) 3151–3164.
[47] J.P. Holman, Experimental Methods for Engineers, eigth ed., The McGraw-Hill, New York, NY, 2011.